Turing-Like Patterns Revisited:
A Peek Into The Third Dimension

Martin Skrodzki* and Konrad Polthier

AG Mathematical Geometry Processing, Freie University Berlin

Arnimallee 6, 14195, Berlin, Germany

{martin.skrodzki,konrad.polthier}@fu-berlin.de

Abstract

Beginning with their introduction in 1952 by Alan Turing, Turing-like patterns have inspired research in several different fields. One of these is the field of cellular automata, which have been utilized to create Turing-like patterns by David A. Young and others. In this paper we provide a generalization of these patterns to the third dimension. Several visualizations are given to illustrate the created models.

Historical Introduction: Turing's Chemical Basis Of Morphogenesis

In 1952, the English Mathematician Alan Turing (June 23, 1912 – June 7, 1954) proposed a model of stable patterns generated by a system of two chemicals, respectively morphogens [10]. The goal was to explain skin patterns of vertebrates, see Figure 1a. The two chemicals, an activator and an inhibitor, diffuse through some substrate and react with each other. While the activator is acting in a short radius around the cell and stimulates the generation of colored pigments, the inhibitor prevents this generation within an annulus of larger radius around the cell.

Given morphogens X and Y with concentration X_r and Y_r in cell r, cell-to-cell diffusion of X called μ and of Y called ν, increase of X given by $f(X, Y)$ and increase of Y given by $g(X, Y)$, Turing proposes the following reaction-diffusion system:

$$\frac{dX_r}{dt} = f(X_r, Y_r) + \mu(X_{r+1} - 2X_r + X_{r-1}), \qquad \frac{dY_r}{dt} = g(X_r, Y_r) + \nu(Y_{r+1} - 2Y_r + Y_{r-1}), \qquad (1)$$

with $r \in \{1, \ldots, N\}$. Here, the cells are arranged in what Turing calls a "ring system".
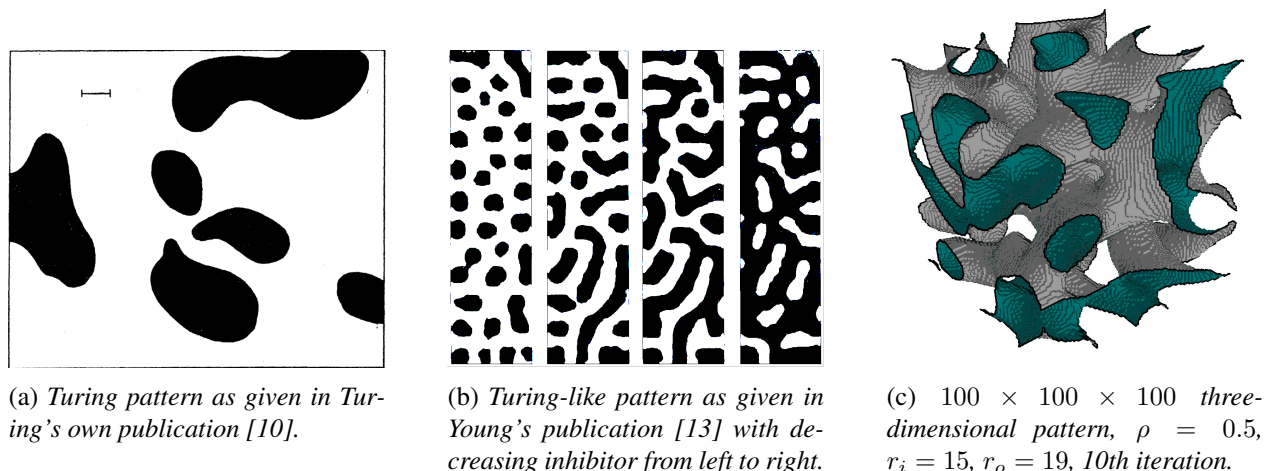
This model inspired many follow-up papers, even up to very recent research [5]. See also the introduction in [4] for a discussion of the reception of Turing's model. Finally, Turing-like patterns are a regular topic at Bridges conferences. Starting with a paper by Jonathan McCabe in 2010 [7], they inspire a seemingly endless flow of fantastic ideas and artworks, see e.g. [4, 9, 11].

Continuing The Story: Young's Vertebrate Skin Patterns

In his 1984 paper "Vertrebrate Skin Patterns" [13], David A. Young builds on the idea of Turing and some extensions by Swindale. He considers the generalized diffusion equation (cf. to Turing's formula (1)):

$$\frac{\partial M}{\partial t} = \nabla \cdot (D \cdot \nabla M) - KM + Q, \qquad (2)$$

where $M = M(r, t)$ is the morphogen (either inhibitor or activator) concentration and the other terms describe diffusion, chemical transformation, and production of the respective morphogen. Every activated cell produces the two morphogens which then diffuse away from the cell, following (2).

(a) *Turing pattern as given in Turing's own publication [10].*

(b) *Turing-like pattern as given in Young's publication [13] with decreasing inhibitor from left to right.*

(c) $100 \times 100 \times 100$ *three-dimensional pattern,* $\rho = 0.5$, $r_i = 15$, $r_o = 19$, *10th iteration.*

Figure 1: *First patterns by Turing and Young, next to a three-dimensional pattern.*

The process is now discretized as a cellular automaton (CA). See e.g. [12] on the topic of CA and confer with the famous "Game of Life" by John Conway as presented e.g. by Martin Gardner [3]. Initially, each cell is randomly activated with some probability $\rho \in [0, 1]$. Young proposes two different kernels for the reaction-diffusion step. The first kernel is circular, while the second kernel has elliptical shape.

We will only discuss the circular kernel here. It is determined by two radii r_i and r_o. The first radius determines an inner, the second an outer circle. During one step of the simulation, all activated cells within the inner circle are counted. They contribute a weight of $+1$ to the currently considered cell. Furthermore, all activated cells lying in the outer, but not in the inner circle, are counted. They contribute a weight of -1. If the overall weight for the current cell is larger than 0, the cell becomes active in the next iteration. Otherwise, it becomes inactive.

In the two-dimensional case, the status $s_{t+1}(C)$ of a given cell $C = (x, y)$ at time $t + 1$ is therefore computed from the weights of its active neighboring cells $C_i = (x_i, y_i)$ at time t by

$$s_{t+1}(C) = \begin{cases} 1 & \sum_i \omega_t(C_i) > 0 \\ 0 & \sum_i \omega_t(C_i) \leq 0 \end{cases}, \quad \text{where} \quad \omega_t(C_i) = \begin{cases} 0 & (x - x_i)^2 + (y - y_i)^2 > r_o^2 \\ 1 & (x - x_i)^2 + (y - y_i)^2 \leq r_i^2 \\ -1 & \text{otherwise} \end{cases} . \quad (3)$$

Note that in Young's original paper, equation (3) is given differently, as ω takes values $1, k, 0$ on the inner disk, its annulus and the outside cells respectively, with k a negative constant.

Generalization To 3D: Volumetric Patterns

In this section we will present our generalization of Young's model to the third dimension. The main idea is to add a term $(z - z_i)^2$ in the right hand side of equation (3). Similar patterns have appeared in medical context [1], when studying reaction-diffusion systems there. They also arose when studying nonlinear phenomena in a physical context [6]. In contrast to these applied works, we focus on an efficient generation of these patterns, providing a variety of different initial conditions. All images shown are created with an approach of CA implementations given by [2] and are therefore highly efficient. As in two dimensions, a stable pattern emerges after a very low number of iterations (10-15). The models are visualized in the JavaView framework [8]. Different steps in the iterative process of the generation of our three-dimensional Turing-like patterns is shown in Figure 2. The variation of parameters r_i and r_o is shown in Figure 3.

(a) *Iteration 1*   (b) *Iteration 2*   (c) *Iteration 3*   (d) *Iteration 10*
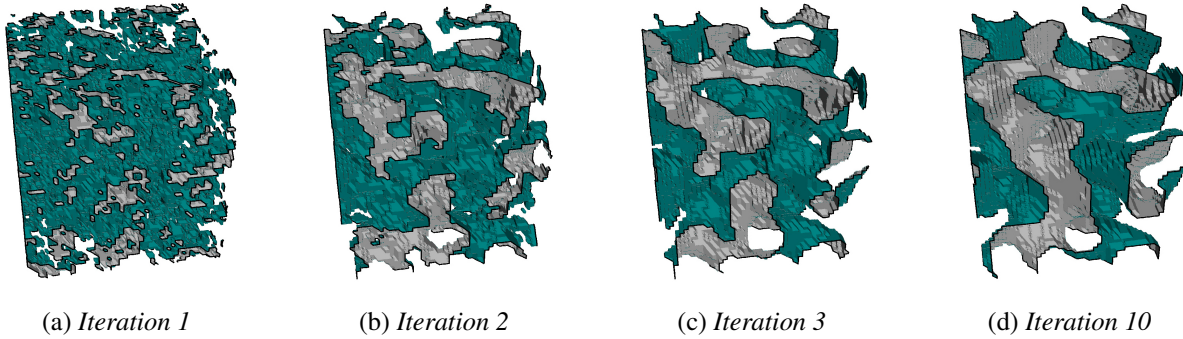
Figure 2: *Iterations of a* $50 \times 50 \times 50$ *cell model with* $\rho = 0.5$, $r_i = 8$, $r_o = 10$.

In the two-dimensional patterns of Figure 1a, 1b, activated cells are colored black, while non-active cells are white. For the visualization of three-dimensional patterns, we chose a different approach. The images show only the boundary between active and non-active cells. It is visualized via the Marching Cubes algorithm, therefore the images look jagged. The darker teal indicates that this side of the boundary has activated cells, while the lighter gray side has non-active cells. For colored versions of the images, we refer the reader to the electronic version of this article. Furthermore, in the two-dimensional patterns, opposing sides of the CA are identified to form a torus on which the simulation is run. The same is performed in 3D, where we identify the opposing sides of a cube to create the images on a three-torus.

Note how in Figure 1b, with varying parameters, the pattern performs a phase transition from disconnected points ("zero-dimensional") to connected stripes ("one-dimensional"). A similar behavior is exhibited by three-dimensional patterns, as shown in Figure 4. One would expect that in three-dimensional patterns also "two-dimensional" connections occur. However, we have not been able to come up with a parameter-set creating these. Hence, they are left for further research.

(a) $r_i = 4$, $r_o = 5$ (b) $r_i = 8$, $r_o = 10$ (c) $r_i = 12$, $r_o = 15$
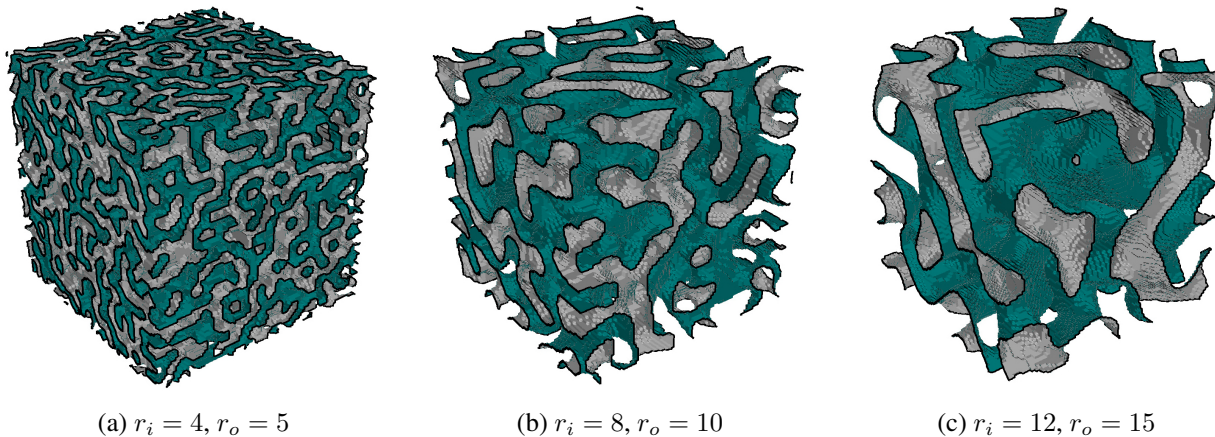
Figure 3: *The respective 10th iteration of three* $100 \times 100 \times 100$ *cell models with* $\rho = 0.5$ *and varying* r_i *and* r_o *parameters. Note the decreasing complexity and also compare to the* $r_i = 15$, $r_o = 19$ *model in Figure 1c.*
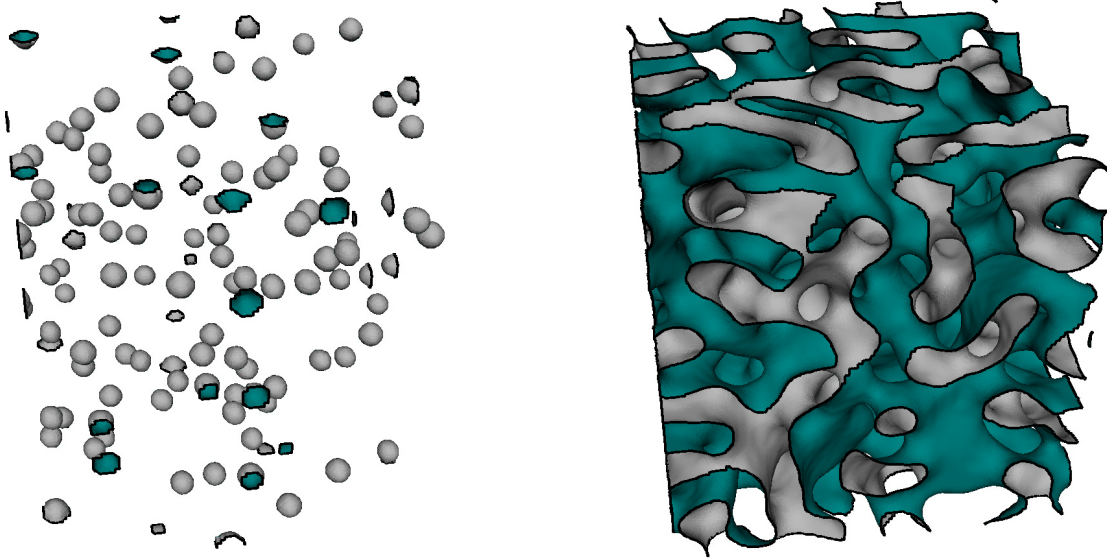
(a) *A $100 \times 100 \times 100$ model exhibiting disconnected points. $\rho = 0.9999, r_i = 4, r_o = 7$, 10th iteration.*

(b) *A $100 \times 100 \times 100$ model exhibiting one-dimensional connection. $\rho = 0.5, r_i = 8, r_o = 10$, 10th iteration.*

Figure 4: *Different connectivities in three-dimensional patterns. Both models have undergone Laplacian Smoothing with fixed boundary to reduce the jagged artifacts of the Marching Cube Algorithm and thus make them aesthetically more pleasant. Note the very high value of ρ in the left pattern, which is due to increased dimension.*

References

[1] Tamás Bánsági, Vladimir K. Vanag, and Irving R. Epstein. Tomography of reaction-diffusion microemulsions reveals three-dimensional Turing patterns. *Science*, 331(6022):1309–1312, 2011.

[2] Allen B. Downey. *Think complexity: complexity science and computational modeling*. " O'Reilly Media, Inc.", 2012.

[3] Martin Gardner. Mathematical games: The fantastic combinations of John Conways new solitaire game "life". *Scientific American*, 223(4):120–123, 1970.

[4] Gary R. Greenfield. Turing-like Patterns from Cellular Automata. In *Proceedings of Bridges 2016: Mathematics, Music, Art, Architecture, Education, Culture*, pages 151–158. Tessellations Publishing, 2016.

[5] Shigeru Kondo. An updated kernel-based Turing model for studying the mechanisms of biological pattern formation. *Journal of Theoretical Biology*, 414:120 – 127, 2017.

[6] Teemu Leppänen, Mikko Karttunen, Kimmo Kaski, Rafael A. Barrio, and Limei Zhang. A new dimension to Turing patterns. *Physica D: Nonlinear Phenomena*, 168169:35 – 44, 2002.

[7] Jonathan McCabe. Cyclic Symmetric Multi-Scale Turing Patterns. In *Proceedings of Bridges 2010: Mathematics, Music, Art, Architecture, Culture*, pages 387–390. Tessellations Publishing, 2010.

[8] Konrad Polthier, Samy Khadem, Eike Preuss, and Ulrich Reitebuch. Javaview home page, 2017. `www.javaview.de`.

[9] Markus Schwehm. A Fast Algorithm for Creating Turing-McCabe patterns. In *Proceedings of Bridges 2016: Mathematics, Music, Art, Architecture, Education, Culture*, pages 431–434. Tessellations Publishing, 2016.

[10] Alan M. Turing. A theory of morphogenesis. *Phil. Trans. B*, 12, 1952.

[11] Andrew Werth. Turing patterns in photoshop. In *Proceedings of Bridges 2015: Mathematics, Music, Art, Architecture, Culture*, pages 459–462. Tessellations Publishing, 2015.

[12] Stephen Wolfram. *A new kind of science*, volume 5. Wolfram media Champaign, 2002.

[13] David A. Young. A local activator-inhibitor model of vertebrate skin patterns. *Mathematical Biosciences*, 72(1):51–58, 1984.